



Paint it Black – To Protect the Qubits

- Reducing Quasiparticle Generation in Superconducting Circuits

*Bachelor Thesis in Engineering Physics & Chemical Engineering with
Engineering Physics*

MATTIAS FREDRIKSSON

HENNING HOLMGREN

SIMON SVENSSON

Department of Microtechnology & Nanoscience

Quantum Device Physics

CHALMERS TEKNISKA HÖGSKOLA

Gothenburg, Sweden 2012

Abstract

This thesis deals with reducing quasiparticle generation in superconducting circuits caused by stray photons by utilizing electromagnetic absorbers. Quasiparticle generation is a known problem in several superconducting circuit applications such as quantum computing research. In order to quantify successful radiation reduction, a superconducting resonator was used as a sensor and a cylindrical shield was designed for testing the absorbers. Four different absorbers were tested, three of them are commercially available microwave absorbers and one was designed by our group. Internal differences were observed between the absorbers, however, compared to reference measurements, no improvements were observed. The results also indicates that the resonators properties changed in-between measurements and more tests should be performed in order to draw final conclusions.

Sammanfattning

Detta projekt behandlar reducering av kvasipartiklar i supraledande kretsar vilka har sin uppkomst i elektromagnetisk strålning. För att reducera denna strålning används elektromagnetiska absorbenter. Alstring av kvasipartiklar är ett känt problem för applikationer där supraledande kretsar ingår, såsom forskning inom kvantdatorer. För att kunna kvantifiera en lyckad strålningsreduktion används en supraledande resonator vars syfte är att agera sensor och en cylindrisk sköld togs fram för att testa absorbenterna. Fyra olika absorbenter användes, tre av dessa är kommersiellt tillgängliga och en togs fram av vår grupp. Interna skillnader för de olika absorbenterna observerades, men i jämförelse med referensmätningar kunde inga förbättringar observeras. Resultaten indikerar även att resonatorns egenskaper förändrades mellan mätningarna och fler tester måste genomföras innan några definitiva slutsatser kan dras.

Contents

1	Introduction	1
1.1	Background and motivation	1
1.2	Purpose	2
1.3	Problem	2
1.4	Method	3
2	Theory	4
2.1	Superconductivity	4
2.1.1	Basics of superconductors	4
2.1.2	Quasiparticles and the superconducting gap	5
2.2	Reaching sub-kelvin temperatures	6
2.3	Resonators	7
2.3.1	Basics of resonators	7
2.3.2	Loaded and unloaded quality factors	8
2.3.3	Overcoupled and undercoupled systems	8
2.3.4	Reflection coefficient	11
2.3.5	Quasiparticle influence on resonator quality factor	11
2.4	Fitting functions	12
2.4.1	Lorentzian function	12
2.4.2	Advanced fitting function	13
2.5	Absorbers	14
3	Experimental Setup	16
3.1	Sample box	16
3.1.1	Assembly	16
3.1.2	Preparation of the resonator	18
3.1.3	Design and assembly of shield	18
3.2	Measurement setup	20

3.3	Applying the absorbers	23
3.3.1	Absorbers 1 & 2, ECCOSORB MCS-U-SA & ECCOSORB GDS-U-SA	23
3.3.2	Absorber 3, ECCOSORB 300	23
3.3.3	Absorber 4, Magic Mix "Black Hole"	24
4	Results	25
4.1	Niobium nitride resonator	25
4.2	Niobium resonator	29
5	Discussion and Conclusion	33
5.1	Discussion	33
5.2	Conclusion	34
6	Acknowledgments	35
	References	36
A	Detailed information	38
A.1	Component register	38
A.2	Niobium resonator recipe	38
A.3	Derivation of the advanced fitting function	39
B	Sammanfattning av kandidatarbete Paint it Black	41
B.1	Introduktion	41
B.2	Teori	42
B.2.1	Resonatorer	42
B.2.2	Absorbenter	42
B.3	Experiment	43
B.4	Resultat och diskussion	44
B.5	Slutsats	44
C	Data sheets	45

Chapter 1

Introduction

1.1 Background and motivation

Quantum computing is a hot topic in modern research and constructing a good qubit architecture is a key point towards a scaled up quantum computer. A qubit represents a unit of quantum information and takes advantage of the fact that it can assume the values $|0\rangle$, $|1\rangle$ or any quantum superposition of these states, whereas a classical bit can only assume the discrete values of 0 and 1, separately. Quantum computers using qubits can theoretically solve some problems much faster than their classical counterparts and several quantum algorithms have already been developed. Qubit structures can be realized in several different ways using any two-level quantum system. For example, the spin of a electron where spin-up would represent 0 and spin-down 1, or a multi-level quantum system, such as an anharmonic oscillator with two states being effectively detached from the rest. The problem lies in the fact that when a quantum system interacts with its environment, it decoheres and lose its quantum properties. Various noise sources, such as electromagnetic radiation, contribute negatively to the coherence time of the qubit, and it turns out that by reducing these noise sources through various means, one can improve the coherence time significantly. A recent experiment conducted at IBM shows that by simply placing the qubit in a mold and submerging it in epoxy, the coherence time of the qubit improved by an order of magnitude[3].

Successful reduction of the radiation that interferes with the qubit will assist in developing more stable qubit architectures which exhibit longer coherence times and hopefully other positive properties as well.

1.2 Purpose

The aim of this study is to protect superconducting qubits from external radiation by developing a recipe for a radiation absorbing paint or finding a commercially available absorber, and also developing a setup for optimized shielding of the sample. The goal is that this study will aid advancements in the field of superconducting qubit research, specifically increasing the coherence time of superconducting qubits. Successful development of an electromagnetic absorber has several application purposes and is not limited to increasing qubit coherence times. In fact, any field suffering from stray photons could benefit from using an electromagnetic absorber.

The project can be divided up into two parts. Part one is to determine what kind of properties the absorber should have in order to come up with some suitable candidates for testing. Obtaining sufficient knowledge in the theory behind qubits and quantum circuits in general, and how they are affected by stray photons is necessary in order to determine the optimal properties of the absorbers. This includes getting familiar with low-temperature physics, microwave theory, and radiation physics.

Part two is to experimentally examine the properties of the absorbers and finding a good radiation absorber that can be used in further superconducting qubit research. It is important to ensure that the absorber survives the low temperature of the cryostat with regard to thermal expansion and that its absorbing qualities are maintained, even at cryogenic temperatures.

1.3 Problem

This thesis will deal with the problem of reducing the influence of stray photons in quantum circuits. The main approach in dealing with this problem will be to use an absorber.

One of the key questions will be to determine which properties the absorber should have and are possible to achieve. It will probably be important for future use of the absorber to decide in which frequency range electromagnetic radiation is most harmful to the qubit. This thesis will include testing the radiation absorption properties of the absorber by measuring the effects on a circuit rather than directly measuring the radiation.

Since the experiments will be conducted at cryogenic temperatures, a part of the problem will be to find an absorber that has a thermal expansion coefficient matching the thermal expansion coefficient of the surface to which it is applied to as closely as possible. Or that it at least won't lose its properties or crack during cooldown, and contaminate the sample.

A limiting factor in comparing different absorbers is the different nature of the absorbers. Some absorbers are solid sheets whereas some are paints or pastes. They can't be applied in the same manner and the ease of removability differs. This combined with the fact that some absorbers are in scarce supply means that different application techniques will have to be used.

Another limiting factor is the time required for one cooldown cycle of the cryostat. This means that the length of the project limits the number of experiments and thus the number of different absorbers and configurations tested.

1.4 Method

To measure the electromagnetic radiation a superconducting resonator will be used. The radiation gives rise to losses in the resonator, which can be used to quantify the level of radiation reaching the sample. The quality of the resonator can be measured and will give an indication of the absorbers' ability to attenuate radiation. The resonator will be placed in a sample box which in turn will be placed in a cylindrical shield. Absorbers will be applied to the sample box or the shield. The entire setup is cooled down in a cryostat.

Chapter 2

Theory

2.1 Superconductivity

In 1908 Heike Kamerlingh-Onnes discovered how to liquify helium. This breakthrough led to cryostats that used helium as a cooling medium. The discovery of liquid He led to a number of interesting observations, one of which was the discovery of superconductivity. In 1911 Kamerlingh-Onnes discovered that the mercury resistor he had attached to the cryostat had dropped significantly in resistance. It would later on be confirmed that it had zero resistance. He conducted several other experiments and by 1914 found that lead and tin had the same characteristics, concluding that the resistance drop in mercury wasn't a measurement error or a property unique to mercury[14].

In 1957, almost 50 years after the first observation of superconductivity, Bardeen, Cooper, and Schrieffer formulated the first microscopical theory for superconductivity; the BCS theory. This theory describes superconductivity as a condensation of paired electrons, Cooper pairs, into a bosonic state [1].

2.1.1 Basics of superconductors

One of the first discoveries in superconductivity was that when a superconductor is cooled down below a certain temperature, its resistance drops abruptly to zero, see figure 2.1. This temperature is called the critical temperature, T_c . All superconductors exhibit this behavior, but different materials have different T_c [15].

In this thesis both niobium (Nb) and niobium nitride (NbN) has been used. Niobium and niobium nitride have critical temperatures around 9.2 K and 14.7 K, respectively[9].

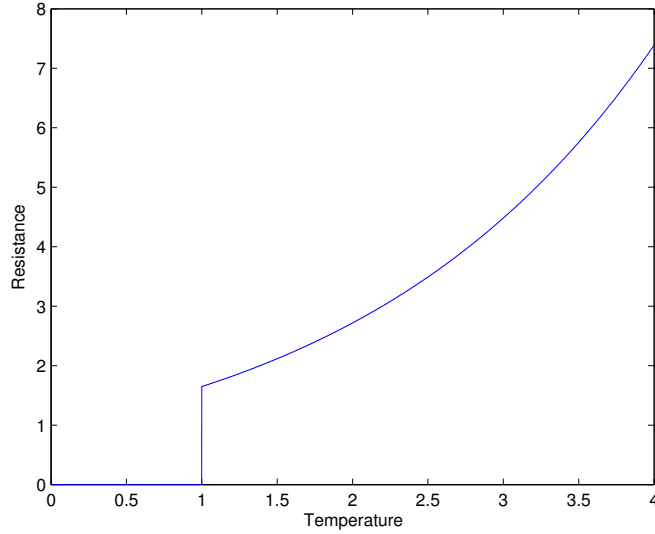


Figure 2.1: The dependence of resistance on temperature. When the temperature drops below a certain value, T_c , the resistance drops to zero.

2.1.2 Quasiparticles and the superconducting gap

Cooper pairs are formed when a material becomes superconducting. Moreover at finite T , there is always a fraction of unpaired electrons or holes. These are called quasiparticles and give rise to losses in the superconducting film[5].

All superconducting materials have a superconducting gap, or energy gap, Δ , which is a material specific parameter. The Cooper pairs are bound to each other by an electron-phonon interaction with an energy shown in equation (2.1), where k_b is Boltzmanns constant[12].

$$2\Delta \approx 3.52k_bT_c \quad (2.1)$$

Therefore, a photon needs an energy $h\nu$, where h is Planck's constant and ν is the frequency, higher than that of the electron-phonon interaction of the Cooper pair, 2Δ in order to break it up. Broken up quasiparticles will recombine back into Cooper pairs after a time $\tau_{qp} \approx 10^{-3} - 10^{-6}s$ [5].

2Δ for niobium is 2.79 meV which corresponds to a electromagnetic wave frequency of 675 GHz. For niobium nitride 2Δ is 4.46 meV with the corresponding electromagnetic wave frequency 1.1 THz. The wavelength, λ , of the photons for these energies is calculated by $E = hc/\lambda$ and gives $444 \mu\text{m}$ and $278 \mu\text{m}$, respectively.

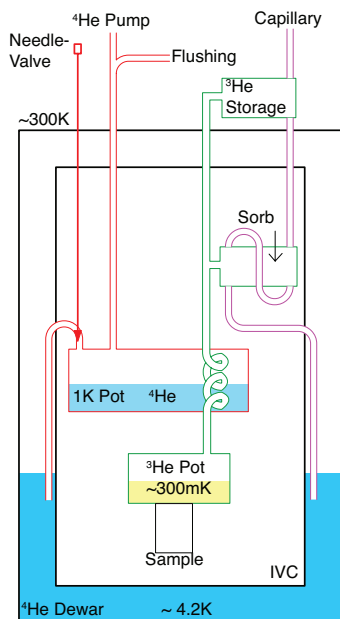


Figure 2.2: A schematic drawing of a typical ^3He cryostat showing the important components.

2.2 Reaching sub-kelvin temperatures

To reach temperatures below 5 K, liquid helium can be used. ^4He liquifies at a temperature of ~ 4.2 K at atmospheric pressure. To lower the temperature further one could lower the pressure with a pump. The reason for this is that when the pressure is lowered helium will evaporate and be pumped out and the only way for the helium to get the energy to evaporate is to take it from the surroundings. The lowest temperature that can be reached by pumping on ^4He is ~ 1 K, but many experiments need to be conducted at substantially lower temperatures.

One way to reach even lower temperatures is to use another helium isotope, ^3He . By pumping on ^3He a temperature of 250 mK can be achieved. The problem with ^3He is that it is extremely expensive and liquifies at a temperature of 3.2 K. One is to use a closed system of ^3He and to lower the temperature in two steps.

A schematic drawing of a typical pumped ^3He cryostat is shown in figure 2.2. The dewar contains the liquid ^4He reserve, blue in the figure. The red lines are the ^4He system, it sucks ^4He from the dewar and the flow is controlled by the needle valve. The red system is connected to a pump that lowers the temperature to about 1.7 – 2.3 K in the 1 K pot. The red system has a heat exchange with the green system that contains the ^3He , which liquifies the ^3He . To pump on ^3He without losing it, a temperature dependent ^3He absorber made out of charcoal is used. It is called the Sorb. When the Sorb is heated, it releases the ^3He and when

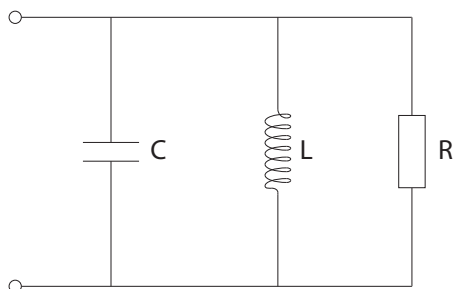


Figure 2.3: Parallel RLC circuit

cooled it absorbs it. By venting ^4He from the dewar through the capillary, see the purple part in the figure, the Sorb is cooled and starts to absorb ^3He , in effect pumping on the ^3He which lowers the temperature of the ^3He pot to 270 – 350 mK.

2.3 Resonators

An intuitive example of a resonator is the pendulum, which oscillate at a given frequency. When systems exhibits resonant behavior, that is, when oscillations around a certain frequency are of a greater amplitude than others, we call them resonators. In this project, resonators are used as sensors by measuring their loss of energy at resonance.

2.3.1 Basics of resonators

Electrical circuits also exhibit resonant behavior at certain frequencies. An analogy to the undamped pendulum with is the LC circuit which consists of an inductance and capacitance connected either in series or parallel. However, dissipation of energy will always occur and the LC circuit is an idealized model. In order to model the damping of the system, a resistance is added to the model, see figure 2.3. The frequency at which the system resonates is given by equation (2.2)[11].

$$\omega_0 = 1/\sqrt{LC} \quad (2.2)$$

Characteristic to all resonators is that around its resonance frequency, the system is able to store energy between cycles very efficiently. However, in order to not break the second law of thermodynamics, some energy will of course be dissipated. In order to quantify these energy losses, it is natural to introduce a quality factor, Q , that describes how much energy is lost during each cycle. We define this quality factor as

$$Q = 2\pi \times \frac{\text{Energy stored in system}}{\text{Energy dissipated per cycle}} \quad (2.3)$$

For high quality factors one can use the definition $Q = f_0/\Delta f$ where f_0 is the resonance frequency and Δf is the Full Width Half Maximum (FWHM) of the resonance peak/dip[11].

However, the quality factor extracted from the circuit model shown in figure 2.3 is an idealized result. In reality, the resonator is coupled to an external system that has a certain input impedance which affect the measured quality factor obtained from measurements performed in a laboratory.

2.3.2 Loaded and unloaded quality factors

The previously mentioned quality factor of the resonator is an inherent characteristic of the resonator itself. In real life applications, the resonator will always “see” an external load caused by the physical coupling of the actual resonator with a transmission line[6]. Thus, the actual quality factor that is measured from the experiments is a combination of the internal quality factor stemming from the resonator and a external quality factor that is related to the measurement setup. The main reason for introducing the external and internal quality factors is to keep track of where the energy losses occur in the system. When modeling the resonator circuit, figure 2.3, with a parallel external load consisting of a coupling capacitance C_c and a impedance Z_0 as shown in figure 2.4, [10], expressions for the external and internal quality factors can be deduced. They are given by equation (2.4) and (2.5)[10].

$$Q_{ext} = \frac{C + C_c}{\omega_0 Z_0 C_c^2} \quad (2.4)$$

$$Q_{int} = \omega_0 R(C + C_c) \quad (2.5)$$

Because this is just a model of the resonator and the lumped circuit elements, shown in figure 2.4, are not actual physical elements but just a representation, it is needed to extract the quality factors experimentally.

2.3.3 Overcoupled and undercoupled systems

As mentioned before, the quality factor is a measure on how good a system is able to store energy between cycles, where a high quality factor indicates low energy losses and a low quality factor indicates high energy losses. Given the internal and external quality factors of a system, one can keep track of where the system is losing its energy. The total quality factor of the system is given by the reciprocal

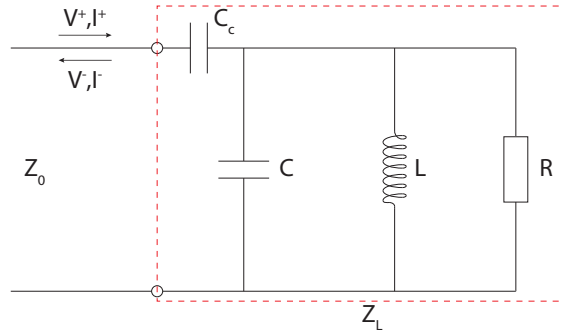


Figure 2.4: Lumped element RLC resonator model.

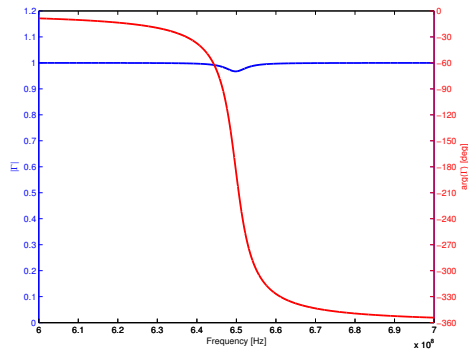
adding of the internal and external quality factors due to the parallel coupling of the resistances [6][10][11].

$$\frac{1}{Q} = \frac{1}{Q_{int}} + \frac{1}{Q_{ext}} \quad (2.6)$$

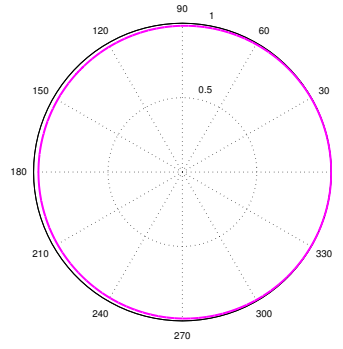
There are three different types of coupling regimes possible in a system when quality factors are defined this way. When $Q_{int} > Q_{ext}$ the system is said to be “overcoupled”. This means that the system is losing more energy via its coupling than inside the resonator itself. If $Q_{int} < Q_{ext}$ the system is said to be “undercoupled” and is losing more energy inside the actual resonator than due to the coupling. In the special case that $Q_{int} = Q_{ext}$ the system is said to be critically coupled.

The different magnitude and phase plots as well as the corresponding polar plots for the different coupling regimes can be observed in figure 2.5. Notice that when the system is overcoupled, the phase of Γ does a 360° wrap, figure 2.5a. In the corresponding polar plot, figure 2.5b, this is represented by a encircling of the origin. In the same manner, if the polar plot does not encircle the origin, the system is in the undercoupled regime, figure 2.5f. As for the critically coupled case, the circle goes through the origin as can be seen in figure 2.5d. Thus we can easily determine the coupling of the resonator by inspection of the polar plot.

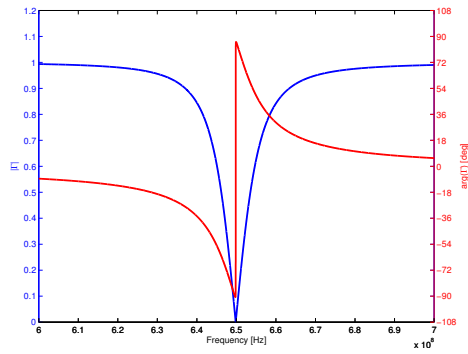
Therefore we want to avoid measuring on a strongly overcoupled system ($Q_{int} \gg Q_{ext}$) which combined with equation (2.6) implies $Q \approx Q_{ext}$ and thus, the measurements wouldn’t tell anything about the resonator’s internal quality factor. If the system is strongly undercoupled, problems will arise as well since the resonance peak will disappear due to large resonator losses. Therefore, a resonator that is as close to the critically coupled regime as possible will be favorable to use.



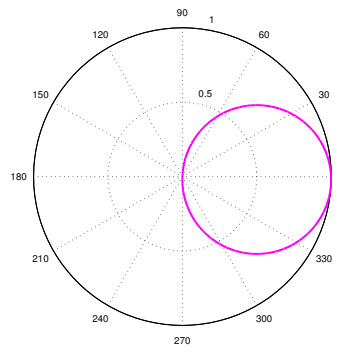
(a) Phase and magnitude of an overcoupled resonator.



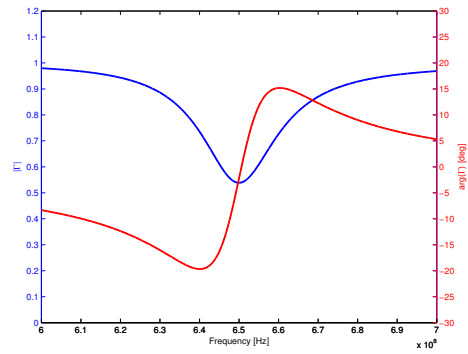
(b) Polar plot of an overcoupled Resonator.



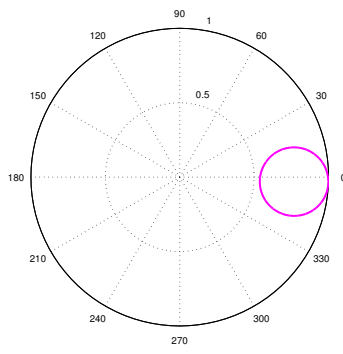
(c) Phase and magnitude of a critically coupled resonator.



(d) Polar plot of a critically coupled resonator.



(e) Phase and magnitude of an undercoupled resonator.



(f) Polar plot of an undercoupled resonator.

Figure 2.5: The phase, magnitude and corresponding polar plot of an overcoupled, a critically coupled and an undercoupled resonator. The plotted function is shown in equation (2.9), with a change in R for the different couplings.

2.3.4 Reflection coefficient

When a signal is sent through a transmission line which is terminated by a system with a certain complex impedance Z_L (i.e. the resonator used), the signal will be reflected back via the transmission line. One can define Γ to be the ratio of the outgoing signal and the incoming signal, such that

$$\Gamma = V^-/V^+ = (Z_L - Z_0)/(Z_L + Z_0) \quad (2.7)$$

Assuming that the resonator is modeled as in figure 2.4, the resonator impedance Z_L is given by

$$Z_L = \frac{1 - \omega^2 L(C + C_c) + j\omega \frac{L}{R}}{j\omega C_c(1 - \omega^2 LC) - \omega^2 C_c \frac{L}{R}} \quad (2.8)$$

By also making the assumption that the transmission line has a purely real impedance such that $Z_0 = R_0$, the expression for Γ becomes

$$\Gamma = (Z_L - R_0)/(Z_L + R_0) = \frac{1 - \omega^2 L(C + C_c(1 - \frac{R_0}{R})) + j\omega(\frac{L}{R} - R_0 C_c(1 - \omega^2 LC))}{1 - \omega^2 L(C + C_c(1 + \frac{R_0}{R})) + j\omega(\frac{L}{R} + R_0 C_c(1 - \omega^2 LC))} \quad (2.9)$$

Using the phase and magnitude information from this expression, the internal and external quality factors can be extracted. This expression will be returned to later.

2.3.5 Quasiparticle influence on resonator quality factor

Quasiparticle generation is known to have significant impact on both superconducting qubit coherence and the quality factor of resonators[2]. A larger quasiparticle density gives rise to shorter coherence times and larger energy losses in resonators. For a resonator with resonance frequency f_0 and quality factor Q , the relation between energy losses and quasiparticle density is given by equation (2.10) [2]

$$\frac{1}{Q} = \frac{\alpha}{\pi} \sqrt{\frac{2\Delta}{hf_0}} \frac{n_{qp}}{D(E_F)\Delta} \quad (2.10)$$

where α is a geometry dependent parameter, Δ represents the superconducting gap for the resonator and $D(E_F)$ is the two-spin density of states at the Fermi energy. Since the experiment is conducted in a cryogenic environment, energy losses in a resonator springing from quasiparticles are expected to vanish due to the fact that the quasiparticle density diminishes exponentially as temperature drops ($n_{qp} \propto \exp[-1/T] \Rightarrow Q \propto \exp[1/T]$). As it turns out, quasiparticle density

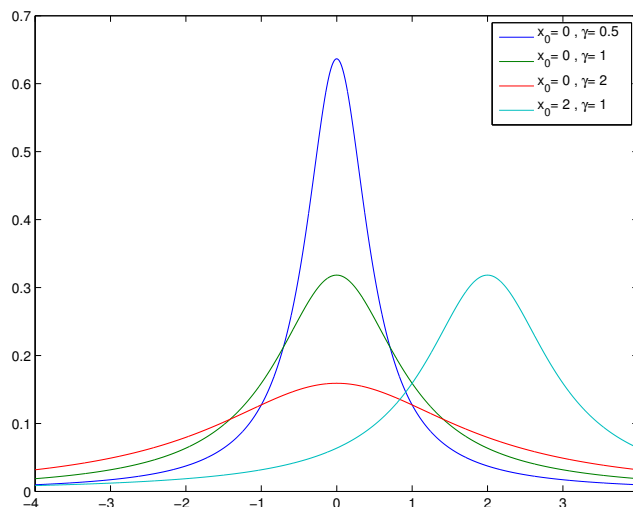


Figure 2.6: The probability functions of the Lorentzian distribution for a few different parameters

does not vanish completely even though the temperature of the surroundings drop to near-absolute-zero temperatures. This suggests the influence of quasiparticle generation due to mechanisms other than thermal excitations. As it turns out, stray photons give rise to quasiparticle excitations as well[2].

2.4 Fitting functions

In order to interpret the data, a function has to be fitted to the data points. Two different fitting functions are used, a Lorentzian to make initial calculations and a more advanced and accurate function for the final calculations.

2.4.1 Lorentzian function

The Lorentzian function is also known as the Cauchy distribution or Lorentz distribution. The probability function describes the amplitude of a resonator over a frequency range, shown in equation (2.11). A Lorentzian can be fitted to the magnitude data as an approximation, which allows to get an estimate of the Full Width Half Maximum(FWHM), f_0 and the total quality factor.

$$f(x; x_0, \gamma) = \frac{1}{\pi} \left(\frac{\gamma}{(x - x_0)^2 + \gamma^2} \right) \quad (2.11)$$

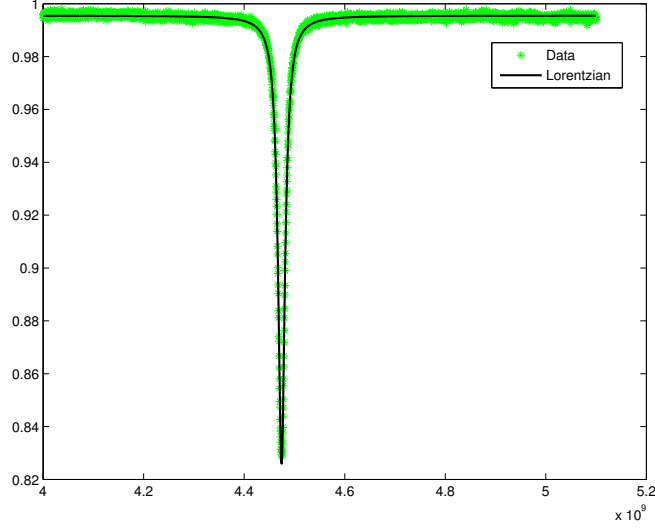


Figure 2.7: Fitting of a Lorentzian to a sample frequency sweep

A plot of the probability density function(PDF) of the Lorentzian distribution for a few sample parameters can be seen in figure 2.6. Fitting a Lorentzian to a sample measurement results in figure 2.7.

The parameters corresponds as follows, x_0 is the point of the peak, which equals the resonator frequency for a resonator if the magnitude is plotted against the frequency. γ is equal to the interquartile range, half width half maximum, which means that 2γ is the Full Width Half Maximum (FWHM). The amplitude is given by the $1/(\pi\gamma)$. This means that if a Lorentzian is fitted to the data from a frequency sweep the quality factor is given by the parameters of the Lorentzian as given by equation 2.12.

$$Q_{total} = \frac{x_0}{2\gamma} \quad (2.12)$$

2.4.2 Advanced fitting function

To gain more information from the measurement data, both the phase and magnitude has to be considered and fitted simultaneously. The Vector Network Analyzer(VNA) measures the S_{11} scattering parameter, also known as the reflection coefficient Γ . Above, equation (2.9) relates the reflection coefficient with the lumped element model of the resonator. Observing the resonator close to the resonance frequency ω_0 , ω can be approximated as ω_0 . With expression (2.5) and (2.4) the reflection coefficient can now be described as equation (2.13)[10], where

$$k = C_c / (C + C_c)$$

$$\Gamma = \frac{k(Q_{ext} - Q_{int}) - j}{k(Q_{ext} + Q_{int}) + j} \quad (2.13)$$

This expression is only valid at the resonance frequency. If in equation (2.9) $\omega_0 + \delta\omega$ is chosen instead of ω where $\delta\omega$ is a small deviation from the resonance frequency, we obtain the expression seen in equation (2.14) for the reflection coefficient. For derivation see appendix A.3.

$$\Gamma = \frac{\delta\omega - j \left(\frac{\omega_0}{2Q_{int}} - \frac{\omega_0}{2Q_{ext}} \right)}{\delta\omega - j \left(\frac{\omega_0}{2Q_{int}} + \frac{\omega_0}{2Q_{ext}} \right)} \quad (2.14)$$

The measurement data is fitted to equation (2.14) with Q_{ext} , Q_{int} , and ω_0 as fitting parameters. The fitting is performed on a slice around the resonance frequency for every frequency sweep during the temperature sweep. In addition to the fitting function, a parameter for the offset of the magnitude and two parameters for the phase shift over the frequency range are used to obtain a good fit.

2.5 Absorbers

When designing an electromagnetic absorber, there are some parameters that need to be considered for optimal performance.

When a EM wave is propagating through free space and strikes the surface of another medium, some reflection will be inevitable. The general form for the reflection coefficient is given by $\Gamma = (Z - Z_0) / (Z + Z_0)$ where $Z_0 = \sqrt{\mu_0 / \epsilon_0} \approx 377 \Omega$ is the impedance of free space and Z is the impedance of the medium that the EM wave impinges on[13]. Similarly, the impedance of the medium is given by $Z = \sqrt{\mu / \epsilon}$ where $\epsilon = \epsilon' - i\epsilon''$ denotes the complex permittivity of the material and similarly, $\mu = \mu' - i\mu''$ is the complex permeability of the material. Given that this is a complex number, it's know that the amount of incident EM radiation that is reflected back is given by the magnitude of Z and the imaginary part introduces a phase shift in the reflected waves.

If one can keep the amount of reflected radiation at a minimum ($Z \approx Z_0$), this means that most of the radiation will enter the medium and be attenuated gradually. The question is now how much the wave will be attenuated once inside the medium, and what parameters that play a role in this attenuation. Assume that the wave is propagating through a lossy, non-conductive medium and that the wave is traveling in the positive x-direction, then Maxwells equations will yield solutions on the form $E_x(z) = E^+ e^{-\gamma z}$ for the forwards traveling wave with $\gamma = \alpha + j\beta = j\omega\sqrt{\mu\epsilon}$ defined as the propagation constant for the medium. α

constitutes the amount of attenuation that the incident radiation will be reduced by. In this case (absorber with high loss and non-conductive), this will be on the form of equation (2.15)[11][13].

$$\alpha = \Re[\gamma] = \omega(\mu^2 \varepsilon'^2 + \tan^2 \delta)^{1/4} \sin \left(\frac{1}{2} \tan^{-1} \left(\frac{\tan \delta}{\mu \varepsilon'} \right) \right) \quad (2.15)$$

In this equation, $\tan \delta = \varepsilon''/\varepsilon'$ is defined as the loss tangent of the materials used. This leads to the second condition for the absorbing material, if the thickness of the absorber is small, then α needs to be large. This means that μ' , μ'' , ε'' and ε' needs to be large. However, an ideal absorber needs the impedance matching condition mentioned in the previous section as well[4].

The surface of the absorbing material could also utilize a rough surface that creates "craters" in order to trap the photons. It has experimentally been shown that if the roughness of the surface is achieved by "large" particles, absorption is at a maximum if the grain size is roughly the same as wavelength of EM radiation[7].

Chapter 3

Experimental Setup

The experimental set-up is made up of three different parts, the sample box and its components, the cryostat and the Vector Network Analyzer (VNA). Each of these must work in order to get any result out of the project.

3.1 Sample box

The sample box is made out of oxygen-free copper and then plated with a thin layer of gold to preserve it from oxidation. The box consists of four parts, see figure 3.1a and consist of two sides, one bottom, and one lid, which are held together by brass screws. The sample box is designed by the quantum devices group at Chalmers MC2 to standardize the experimental setups. It is constructed to fit six SMK connectors and a Printed Circuit Board (PCB). Each part is designed in AutoCAD and manufactured using CNC milling by the MC2 technicians.

3.1.1 Assembly

The connectors for the sample box consists of three parts, see figure 3.1b, with a glass bead being the inner part which is connected to an SMK connector via an adapter. The glass beads are soldered into place in the sample box, see figure 3.2. The glass beads are connected to the PCB by a microwave launcher that is soldered to the PCB and clamped to the glass bead.

When all glass beads are soldered and safely in place inside the sample box, the adapters to the SMK connectors and connectors are attached, see figure 3.3. Five out of six connections are shorted to ground with a grounding cap.

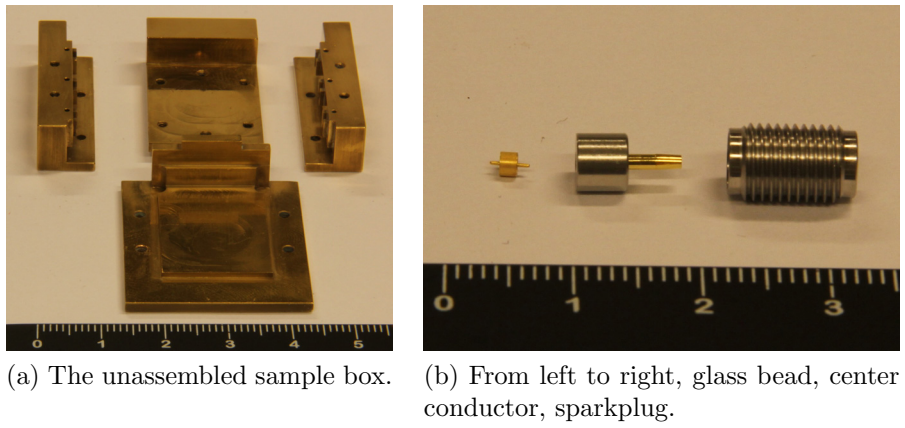


Figure 3.1: All the parts for the sample box before assembly.

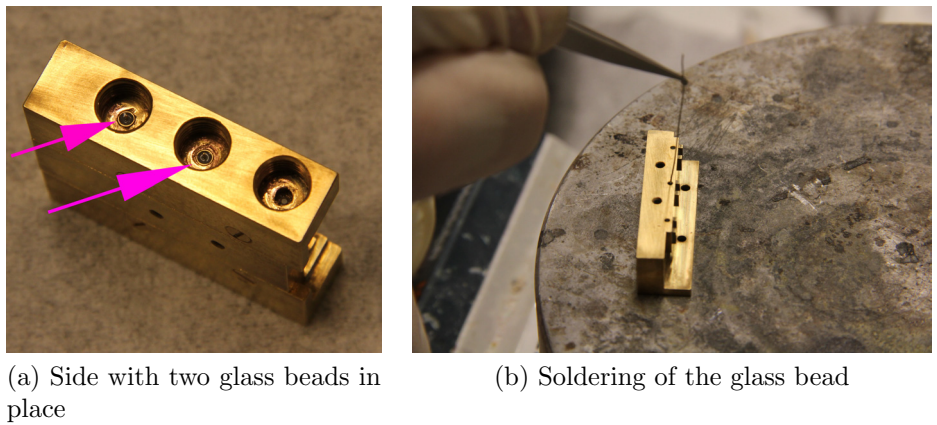


Figure 3.2: Placing the glass beads in the sample box.

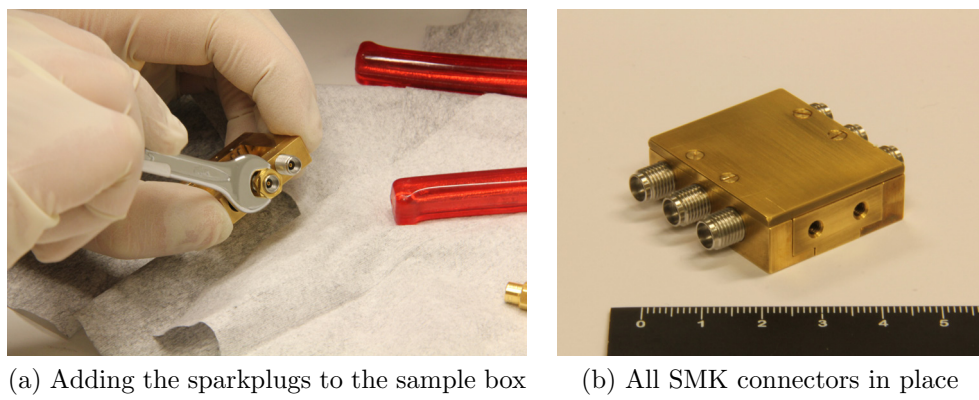


Figure 3.3: Completely assembled sample box

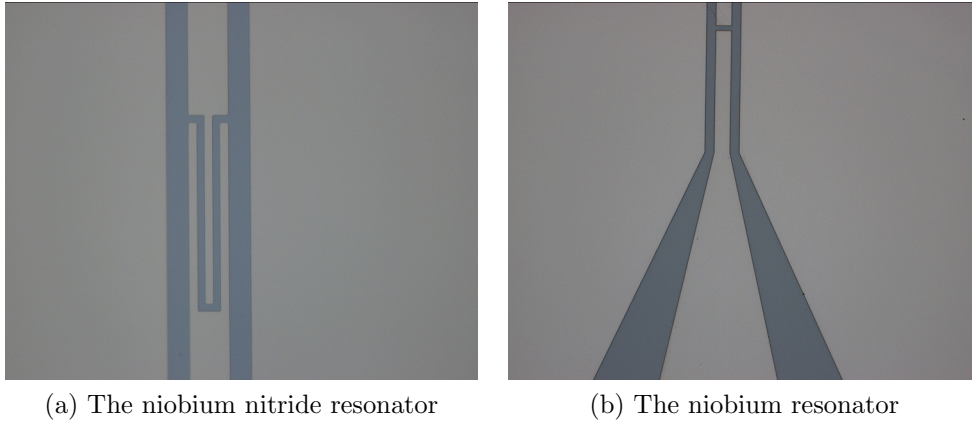


Figure 3.4: Microscope picture of the two resonators. Shown is the coupling capacitance C_c .

3.1.2 Preparation of the resonator

For the experiments a superconducting resonator was used. The resonator was custom fabricated in the clean room at MC2. For a microscope picture see figure 3.4. The resonator is made out of niobium nitride(NbN) on silicon. Later on a second resonator was manufactured out of niobium(Nb), with a lower coupling capacitance value to raise the external quality value. Figure 3.4 shows the difference in capacitor design, figure 3.4a shows the interdigitated design that gives a high capacitance, and figure 3.4b shows capacitor consisting of only a gap, which gives a lower capacitance. Compare this with a normal capacitor where the capacitance is a function of the surface area of the parallel plates. The PCB on which the resonator is mounted is made out of Rogers 3010 with gold plated copper as conductor.

In the next step the resonator is glued onto the PCB. The glue holds the resonator in place and the electrical connection is made by wire bonding the resonator to the PCB by using AlSi wire. Connections are made both for the ground planes and the resonators center conductor.

3.1.3 Design and assembly of shield

The initial plan was to paint the sample box itself, however since many of the paints use epoxy as a binder it was decided not to paint the sample box. Instead a shield was designed to fit around the sample box. The requirements of the shield were that it should be easy and cheap to mass produce, it has to fit the sample box, and it has to fit inside of the cryostat.

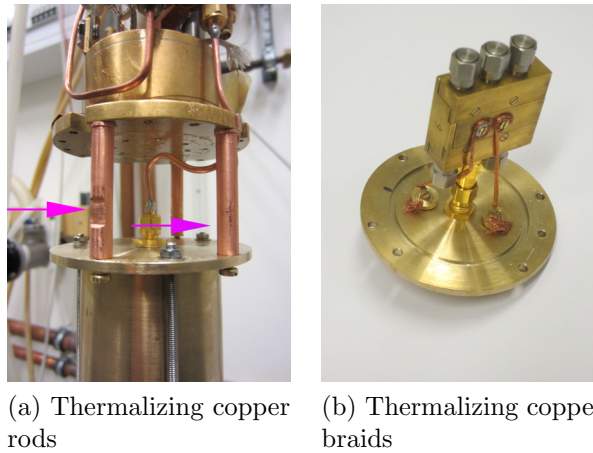


Figure 3.5: Design features of the shield for evacuation and thermalization

Since the shields of the cryostats are shaped cylindrically, it was decided that a cylinder is a good model. It was designed in such a way that the lid was reusable and new cylinders could be used for every experiment. Since brass was available, cheap, and is a good thermal conductor it was chosen as construction material. A CAD model of the setup can be seen in figure 3.7.

The cylinder is milled out of a brass rod and is 77 mm high. In the bottom of the cylinder a small hole is drilled to be able to evacuate the inside.

The lid consists of a plate with a hole in the center that fits the connector. The connector is sealed with indium. On the rim of the lid, three holes are drilled to fit the screws that holds the shield together, and four other holes were drilled such that copper rods could be attached to the shield and the ^3He pot. The rods create a good thermal contact between the ^3He pot and the shield, figure 3.5a. Inside the lid a slot is milled out in which the cylinder fits. An indium seal is applied between lid and cylinder. Two screws were attached to the inner side of the lid for holding copper braids that will thermalize the sample box to the shield, figure 3.5b.

The bottom is the same size as the lid and a slot is milled out in the center that fits the bottom of the cylinder. There is also a small track milled from the center of the bottom to one of the sides, see figure 3.6. This track connects to the hole in the bottom of the cylinder and provide an efficient way to evacuate the shield, however doesn't provide a direct line of sight for stray photons into the shield.

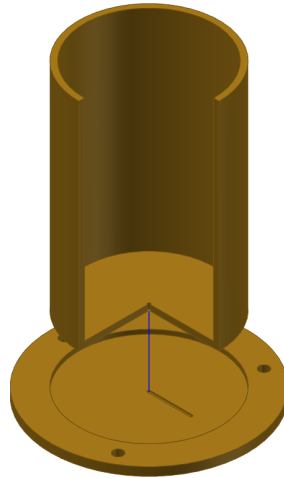


Figure 3.6: Track for evacuating the Shield

3.2 Measurement setup

The experiment is set up with a Vector Network Analyzer (VNA) connected to attenuators on port 1 and amplifiers on port 2, figure 3.8. On the input line several attenuators are connected, attenuating the signal and the radiation in the transmission line to the same level as the surrounding black body radiation through the different temperature stages. The circulator sends the signal from the input line down to the sample and send the reflection up through the output line. On the output line the signal is amplified both with a cold low noise amplifier and three room temperature amplifiers.

The VNA can handle frequencies in the range of 10 MHz to 50 GHz, however the SMK connectors, the coaxial cable and lines in the fridge can only handle up to around 18 GHz. The Low Noise Amplifiers (LNA) being used can only handle frequencies in the range of 4-8 GHz. This is one of the reasons there is a 8 GHz Low Pass filter in the setup.

The base temperature of the cryostat varies between 270 mK and 350 mK. At base temperature a power sweep is performed, to check if the resonator has a power dependency, followed by a temperature sweep.

To do a temperature sweep, the heaters inside the fridge for heating the Sorb as well as dedicated heaters near and in thermal contact with the sample are utilized. They are fed with manually regulated DC power. To increase control of the temperature and in an effort to keep a linear and slow temperature increase, the cooling mechanisms of the cryostat are used in combination with the heating. When cooling on the Sorb or the 1 K Pot at the same time as carefully heating, a quite fine control can be achieved.

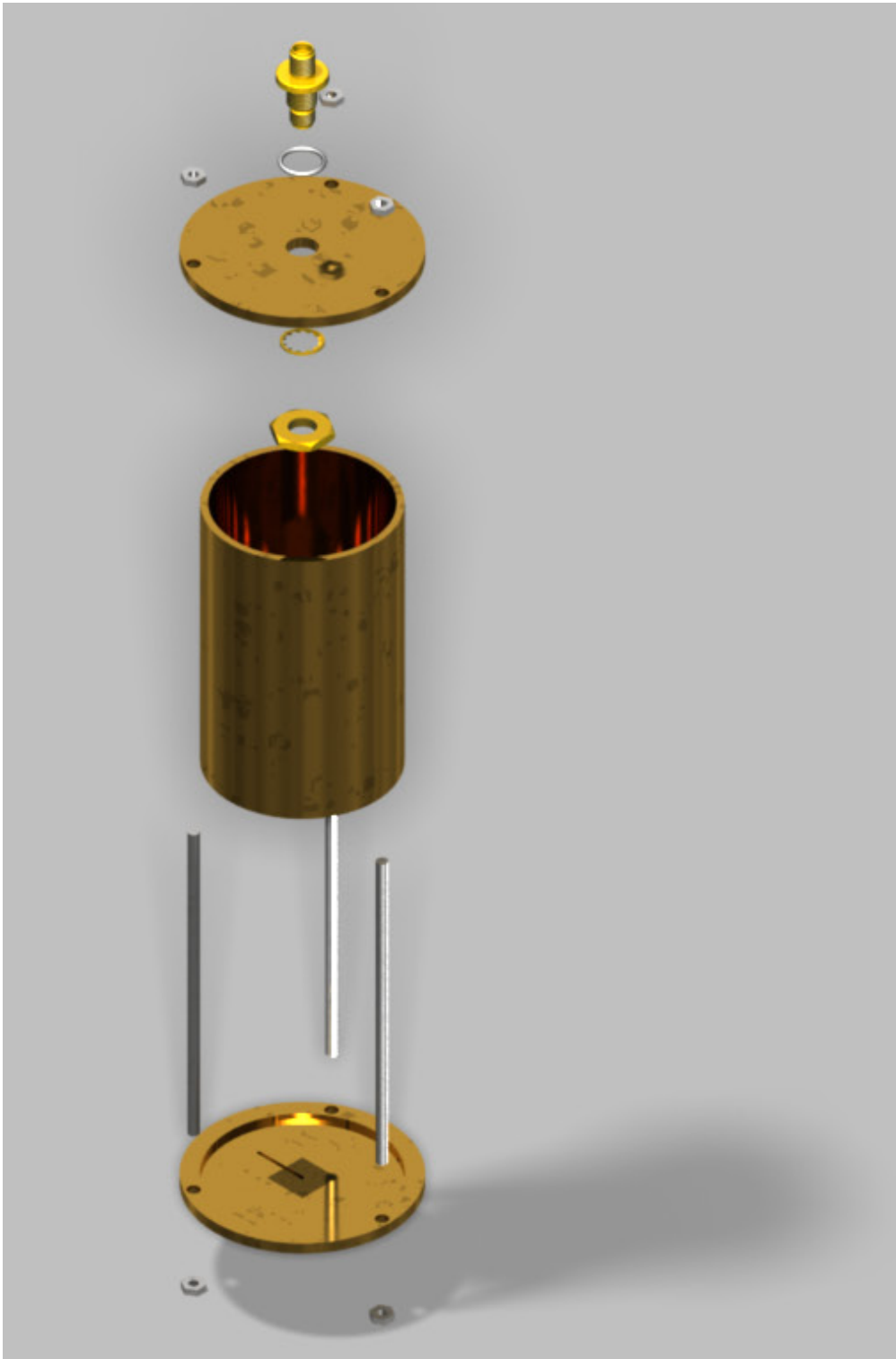


Figure 3.7: 3D CAD model of the shield used for experiments.

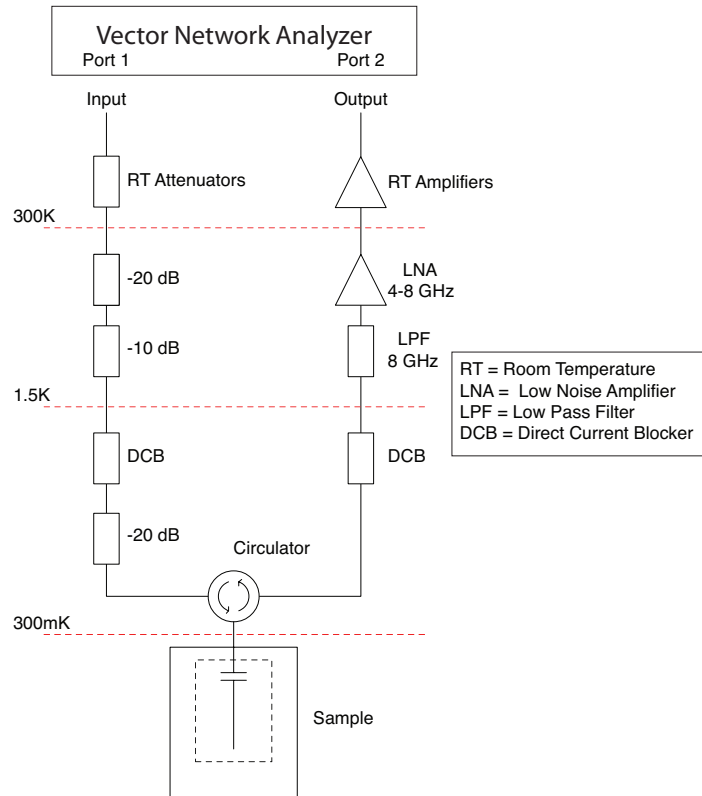


Figure 3.8: The internal electronics of the cryostats measurement lines. Above the 300 K dashed line are room temperature amplifiers and attenuators outside the cryostat.



Figure 3.9: The cylinder shield painted with ECCOSORB 300.

3.3 Applying the absorbers

Four different absorbers have been tested, some have only been tested with the niobium resonator and some have been tested with both.

3.3.1 Absorbers 1 & 2, ECCOSORB MCS-U-SA & ECCOSORB GDS-U-SA

Two cavity resonance absorbers were used, MCS-U-SA and GDS-U-SA. MCS-U-SA is a thin, flexible, high-loss, magnetically loaded, electrically non-conductive broadband absorber. It is designed for the frequency range from 800 MHz to 18 GHz. GDS-U-SA is a thin, flexible, high-loss, magnetically loaded, electrically non-conductive broadband absorber. It is designed for the frequency range from 6 GHz to 35 GHz. None of them were developed specifically for cryogenic temperatures.

The absorbers were cut with a knife to a 1.5×2.4 cm size. The height of GDS is 0.76 mm and for the MCS 1.01 mm. The pieces were then glued onto the inside of the lid. The sample box was sealed and then placed in the cylindrical shield.

3.3.2 Absorber 3, ECCOSORB 300

Eccosorb Coating 300 is a two-part polyurethane lossy absorber coating that is heavily loaded with iron filler. It is a coating that is applied as a paint, in industrial applications it can be applied as a spray. Typical frequency absorption range is 1 GHz and above.

The cylinder is painted several times on the inside to get the required thickness of the absorber, about 2 mm.

Table 3.1: Magic Mix "Black Hole" recipe used on the inside of the shield. The stycast is a 2 part epoxy.

Substance	Weight Percent
Stycast 1266	45%
Carbon Black	5%
Silicon Carbide 46 grit	25%
Silicon Carbide 600 grit	25%



Figure 3.10: The Cylindrical shield painted with the Magic Mix "Black Hole", mixed according to table 3.1.

3.3.3 Absorber 4, Magic Mix "Black Hole"

The Magic Mix "Black Hole" is an absorber adopted by our group. It is based on a recipe developed for spectrometers[7]. This recipe is based on a recipe used in the experiments performed at Santa Barbara[2]. It utilizes large grains to create a rough surface to absorb the millimeter size waves and a carbon black filled stycast epoxy to absorb sub-millimeter waves. It was however not possible to get the exact grain sizes and stycast epoxies. We combined it with a recipe published in Journal of Physics[8] regarding absorbing electromagnetic radiation by impedance matching. The resulting recipe can be seen in table 3.1. The epoxy, Stycast 1266, is a 2 part epoxy mixed as 28 parts B to 100 parts A.

Chapter 4

Results

4.1 Niobium nitride resonator

The niobium nitride resonator, see figure 3.4a, was the first resonator to be used. The measurements performed on the NbN resonator consisted of three different setups, one reference measurement and two measurements with the absorbers, MCS-U-SA and GDS-U-SA, glued to the inside of the sample box lid. See figures 4.4, 4.2, 4.1 and 4.3 for graphs of the measured quality factors and resonance frequency. Notice the similarity in the quality factors for all the setups. Observing the polar plot for the reflection coefficient in figure 4.5, we can see that the NbN resonator is strongly overcoupled and as stated before, this causes problems in drawing conclusions about the absorbers ability of reducing stray photon impact. This might explain the invariance of the measured quality factors.

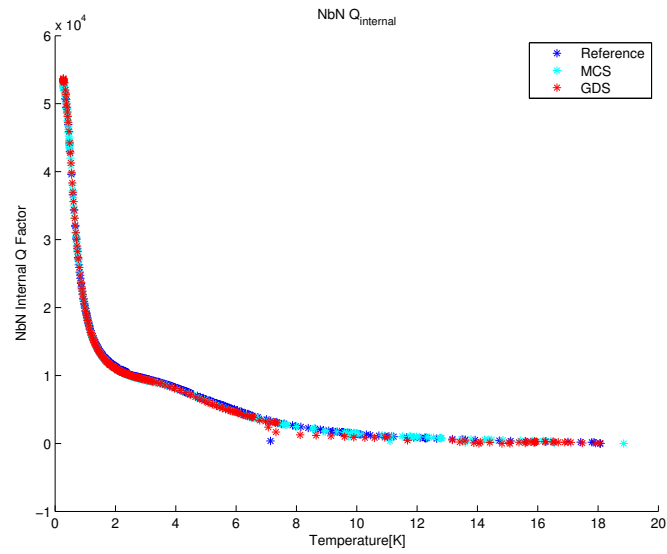


Figure 4.1: Internal quality factor for the NbN resonator as a function of temperature for the different absorbers.

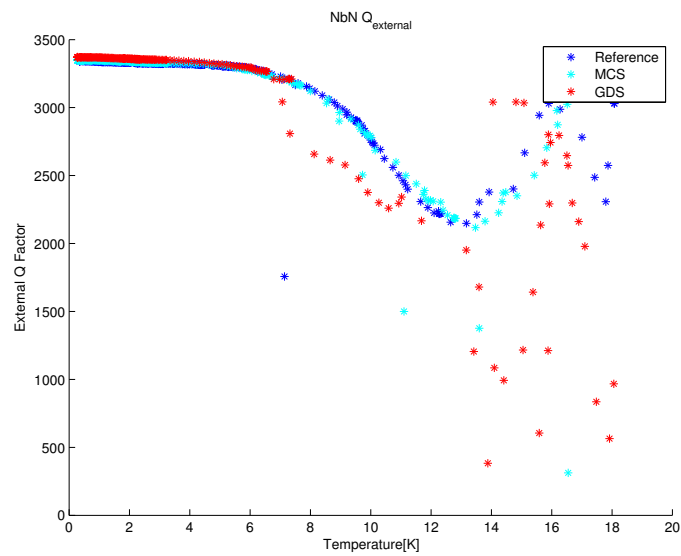


Figure 4.2: External quality factor for the NbN resonator as a function of temperature for the different absorbers.

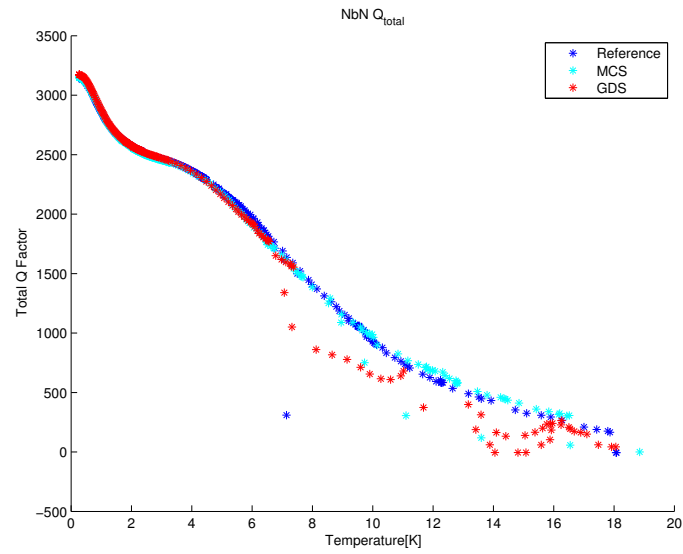


Figure 4.3: Total quality factor for the NbN resonator as a function of temperature for the different absorbers.

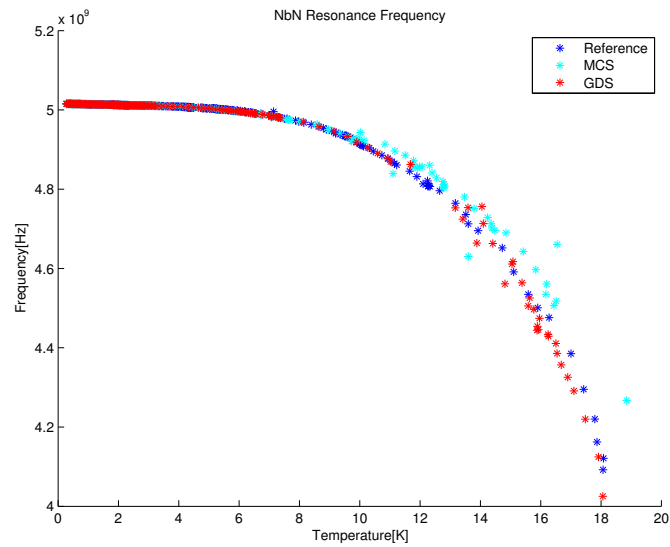


Figure 4.4: Resonance frequency for the NbN resonator as a function of temperature for the different absorbers.

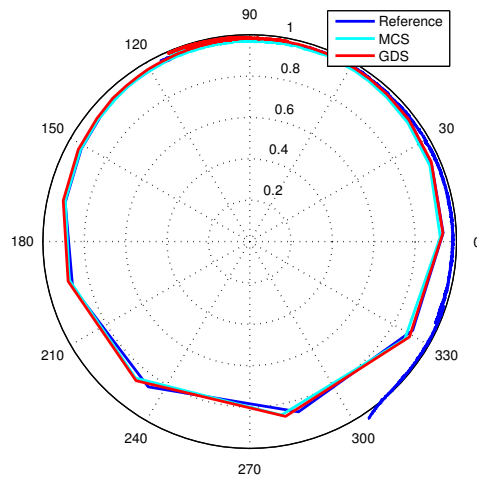


Figure 4.5: A polar plot of a sweep at base temperature showing the difference in coupling for the NbN resonator with different absorbers.

4.2 Niobium resonator

Using the niobium resonator, measurements with the solid absorbers, MCS-U-SA and GDS-U-SA glued to the inside of the lid were performed. Measurements on the ECCOSORB 300 which is a paint that was applied on the inside of the cylinder and the in house made Magic Mix "Black Hole", applied in the same manner, were performed as well.

The results of the measurements are shown in figure 4.9, 4.6, 4.7, 4.8, and 4.11. Figure 4.9 shows the temperature dependence of the resonators resonance frequency for different absorber setups.

Figure 4.6 shows the temperature dependent internal quality factor for the different absorbers as well as for the reference measurement. Note that the reference measurement has the highest internal quality factor, this was an unexpected result since shielding the sample should not lower the quality factor, assuming that the absorber does not interact with the resonator. We can see that the Magic Mix "Black Hole" seems to be the best of the absorbers with ECCOSORB 300 coming in second place.

Figure 4.7 shows the temperature dependent external quality factor for the different absorbers. This should not change with temperature. The fact that the reference, ECCOSORB 300 and Magic Mix has the same external quality factors is as expected. The MCS and GDS absorbers are placed inside the lid and show different external quality factors, this could indicate that it interacts with the resonator.

Figure 4.11 shows a polar plot of a sweep at base temperature. The reference measurement encircles the origin, implying it is overcoupled.

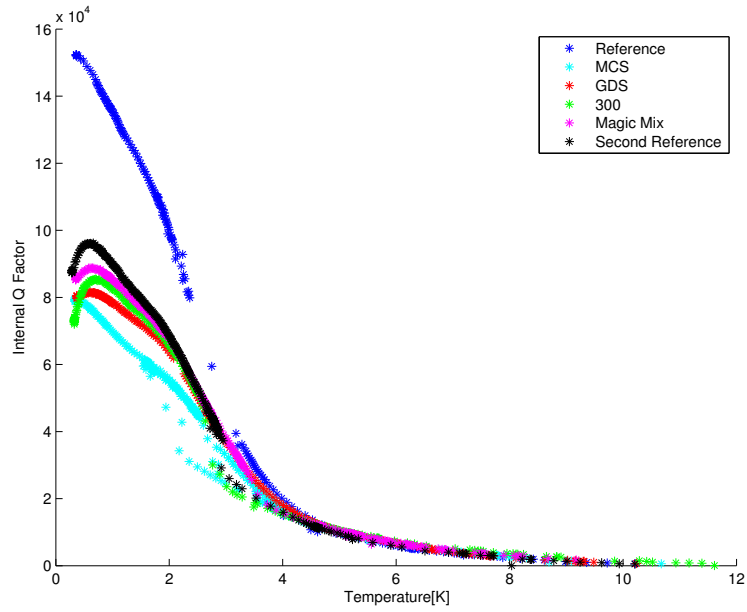


Figure 4.6: Internal quality factor for the Nb resonator as a function of temperature for the different absorbers.

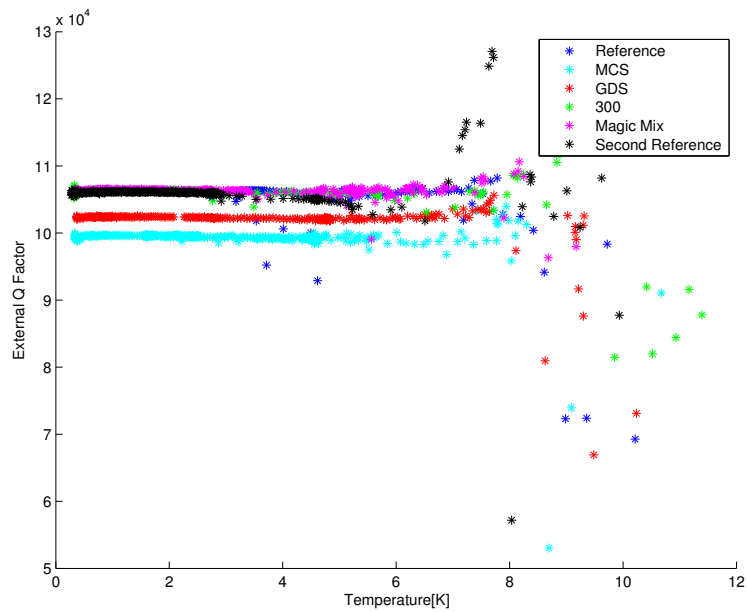


Figure 4.7: External quality factor for the Nb resonator as a function of temperature for the different absorbers.

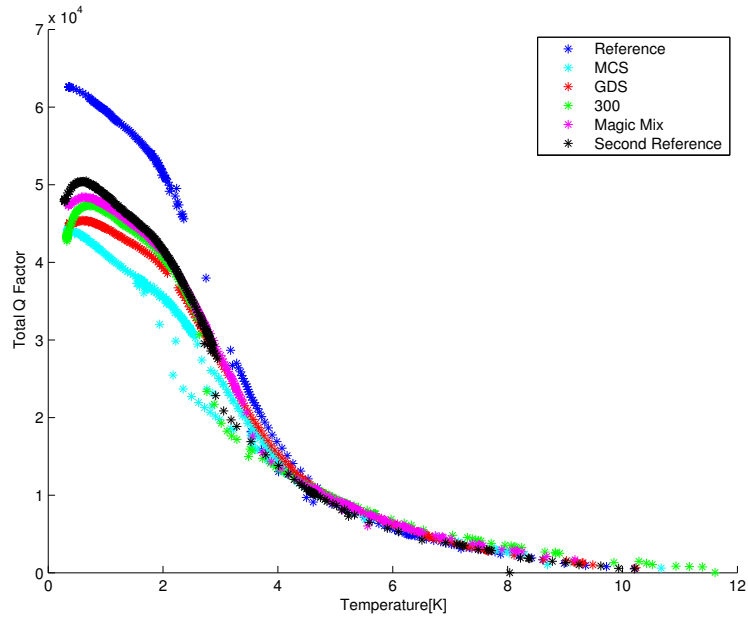


Figure 4.8: Total quality factor for the Nb resonator as a function of temperature for the different absorbers.

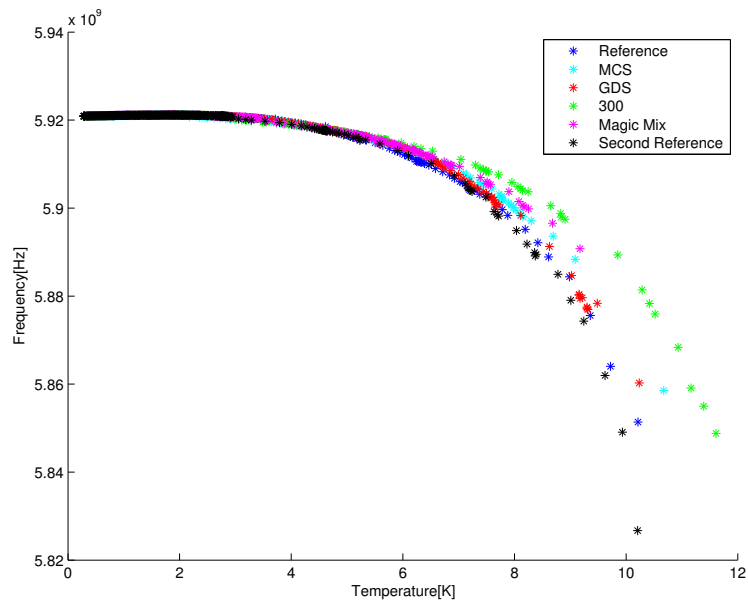


Figure 4.9: The resonance frequency for the Nb resonators as a function of temperature for the different absorbers.

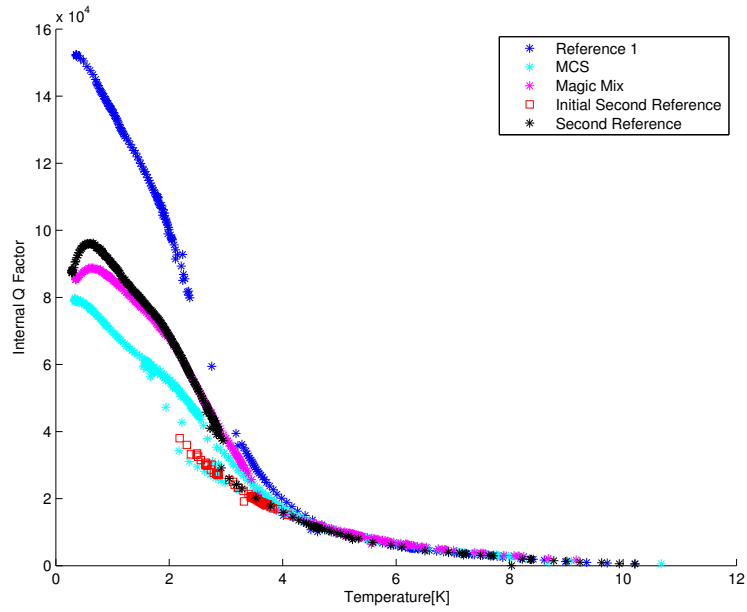


Figure 4.10: The internal quality factor of all the reference measurements on the Nb resonator as well as two of the absorbers

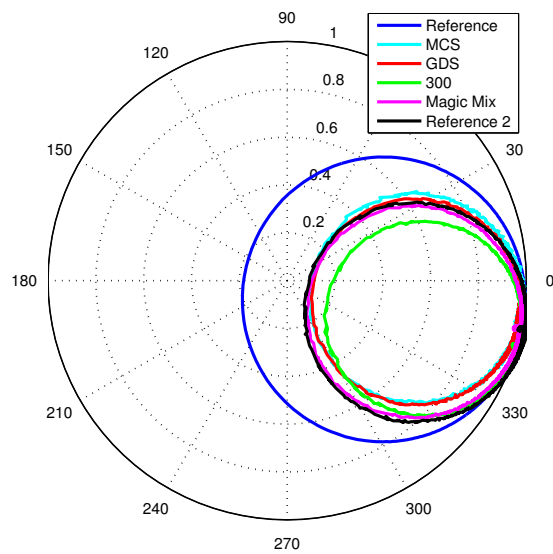


Figure 4.11: A polar plot of a sweep at base temperature showing the difference in coupling for the Nb resonator with different absorbers.

Chapter 5

Discussion and Conclusion

5.1 Discussion

We observe a drop in internal quality factor from the reference measurement in comparison to all of the measurements with absorbers. This was very unexpected. Since the absorbers inside the lid are placed a few millimeters from the resonator it is not extremely far fetched to assume that the resonators coupling capacitance could be affected. This is due to the fact that the absorbers have a different dielectric constant than that of free space, which could alter the effective dielectric environment of the coupling capacitor. Such a change in capacitance however, would change the resonance frequency of the resonator according to equation (2.2), this has not been observed as can be seen in figure 4.9.

For the absorbers applied on the shield, ECCOSORB 300 and the Magic Mix "Black Hole", interaction with the resonator is highly unlikely. This implies that the quality factor should have increased or at least not changed, since the absorption of stray photons should not affect the resonator in a negative way. If the absorbers are inefficient and do not absorb any radiation we should still not see a lower total quality factor. One possibility is that the chip could have been damaged or contaminated in between the reference measurement and the measurements of the absorbers. This contamination or oxidation of the resonator would have changed the internal quality factor.

We decided to make a second reference measurement to try to confirm that the internal quality factor of the resonator had changed. The initial second reference measurement was performed between 2 K and 4 K since the cryostat would not cool down properly. However it implied a trend confirming our suspicions. A complete second reference measurement was performed, however it showed a quality factor higher than all the measurements with absorbers but significantly lower than the first reference measurement, see figure 4.10. This result adds to

the uncertainty since the difference between the two reference measurements have a maximum relative difference of approximately 50%. The difference between the initial second reference and the second reference have also maximum relative difference of approximately 50%. Thermal contact between the IVC and the shield would explain why the cryostat would not cool down, it could also explain the difference between the two second reference measurements.

We can, however, observe internal differences between the absorbers, figure 4.6. The custom made Magic Mix "Black Hole" yields best results, followed by, in descending order, ECCOSORB 300, GDS, MCS. However, since the differences in quality factor between the absorbers are lower by one order of magnitude compared to their respective quality factors, we cannot draw very strong conclusions about their effectiveness.

The measurements of the MCS and GDS absorbers give an external quality factor that does not match the quality factor of the reference and the absorbers applied on the shield, see figure 4.7, note that this difference is small though. This could indicate that they interact electrically with the resonator. The reason for the spread of the high temperature external quality factor is because when the resonance disappears the fit will yield bad results. The fit might be the reason for the difference in external quality factor.

At the beginning of the project a niobium nitride(NbN) resonator was used. When measuring with the NbN resonator we could not see any difference in the quality factor between a shielded and a unshielded sample, figure 4.1. The NbN resonator was very overcoupled, figure 4.5, which means that the main part of the total quality factor consisted of the external quality factor. To observe any change in radiation shielding the internal quality factor is of interest. It was decided to fabricate a new Nb resonator which has a lower superconducting gap and which is also more undercoupled, such that the internal quality factor is dominating the total quality factor.

Part of the initial project was to model the problem with COMSOL. However, it did not pan out well, since the frequencies of interest were much higher than initially believed. This made the problem very hard to model in a precise way. There does not exist any analytic method in deciding optimal absorber placement in cavities[4].

5.2 Conclusion

From the experiments performed we can conclude that the custom made Magic Mix "Black Hole" seems promising. However the effectiveness of the absorbers are inconclusive. More tests should be performed.

Chapter 6

Acknowledgments

We want to express our sincere gratitude to our supervisors, Michaël Simoen and Philip Krantz, who have been encouraging and helping us throughout this project. Lars Jönsson for creating the cylinder shields in which the experiment took place and the invention of the paste application device, Kyle Sundqvist for putting up with stupid questions regarding modeling in COMSOL, Staffan "Ubbe" Nilsson for his proofreading, and the rest of the staff of Quantum Device Physics for helping out. Last but not least, the coffee machines on floor 5 in the MC2 building.

References

- [1] J. Bardeen, L. Cooper, and J. Schrieffer. Theory of superconductivity. *Physical Review*, 108:1175–1204, 1957.
- [2] R. Barends, J. Wenner, M. Lenander, Y. Chen, R. C. Bialczak, J. Kelly, E. Lucero, P. O’Malley, M. Mariantoni, D. Sank, H. Wang, T. C. White, Y. Yin, J. Zhao, A. N. Cleland, J. M. Martinis, and J. J. A. Baselmans. Minimizing quasiparticle generation from stray infrared light in superconducting quantum circuits. *Applied Physics Letters*, 99(11):113507, 2011.
- [3] A. Córcoles, J. Chow, J. Gambetta, C. Rigetti, J. Rozen, G. Keefe, M. Rothwell, M. Ketchen, and M. Steffen. IBM research report protecting superconducting qubits from external sources of loss and heat. *New York*, 25203, 2011.
- [4] P. Dixon. Cavity-resonance dampening. *Microwave Magazine, IEEE*, 6(2):74 – 84, june 2005.
- [5] J. Gao. *The Physics of Superconducting Microwave Resonators*. California Institute of Technology, 2008.
- [6] D. Kajfez. Q factor measurements, analog and digital. Technical report, University of Mississippi, 1999. <http://www.ee.olemiss.edu/darko/rfqmeas2b.pdf>.
- [7] T. Klaassen, J. Blok, J. Hovenier, G. Jakob, D. Rosenthal, and K. Wildeman. Absorbing coatings and diffuse reflectors for the herschel platform sub-millimeter spectrometers hifi and pacs. In *Terahertz Electronics Proceedings, 2002. IEEE Tenth International Conference on*, pages 32 – 35, 2002.
- [8] X. Liu, Z. Zhang, and Y. Wu. Absorption properties of carbon black/silicon carbide microwave absorbers. *Composites Part B: Engineering*, 42(2):326 – 329, 2011.

- [9] B. T. Matthias, T. H. Geballe, and V. B. Compton. Superconductivity. *Rev. Mod. Phys.*, 35:1–22, Jan 1963.
- [10] F. Persson. *Fast Dynamics and Measurements of Single-charge Devices*. Doktorsavhandlingar vid Chalmers tekniska högskola. Chalmers University of Technology, 2010.
- [11] D. Pozar. *Microwave engineering*. Wiley, New York, 3. ed. edition, 2004.
- [12] M. Tinkham. *Introduction to Superconductivity*. McGraw-Hill Inc., 2 edition, 1996.
- [13] X. Tong. *Advanced Materials and Design for Electromagnetic Interference Shielding*. Advanced Materials and Design for Electromagnetic Interference Shielding. CRC Press, 2008.
- [14] D. van Delft and P. Kes. The discovery of superconductivity. *Physics Today*, 63(9):38–43, 2010.
- [15] J. Waldram. *Superconductivity of Metals and Cuprates*. Institute of Physics Pub., 1 edition, 1996.

Appendix A

Detailed information

A.1 Component register

Component name	Model/Order number	Company manufacturing
Glass Bead	K100	Advanced Technology group
Sparkplug	K102F-R	Anristu
AlSi wire	1% Si	Kulicke & Soffa
PCB	Custom made	Hughes Circuit, Inc.
Room temperature attenuator	2AH/18AH (−20 dB)	Aeroflex, Inmet
Short circuit	7008 (SMA, DC-18 GHz)	Aeroflex, Inmet

A.2 Niobium resonator recipe

1. Cleaning wafer
 - HF bath, 2% concentration, 20 s
 - Rinse in DI-water
 - Blowdry with N_2
2. Deposit Nb
 - Sputtering, 120 nm
3. Prepare for electron beam lithography
 - Spin MMA(8,5)EL10, 500 rpm, 5 s, 2000 rpm 45 s
 - Softbake 170 °C, 5 min
 - Spin ZEP520A 1:1 Anisole, 3000 rpm, 1 min

- Softbake 170 °C, 5 min
- 4. Expose resonator pattern
 - 70 nA in e-beam
- 5. Develop ZEP layer
 - o-xylene (96 %), 2 min
 - Rinse in Isopropanol
 - Blowdry with N_2
- 6. Develop EL10 layer
 - H_2O :Isopropanol (1:4), 4 min
 - Rinse in Isopropanol
 - Blowdry with N_2
- 7. Reactive ion etching of Nb
 - CF_4/O_2 (50/10 sccm)
- 8. Spin protective resist
 - Spin S1813, 3000 rpm, 1 min
 - Softbake, 110 °C, 3 min
- 9. Dicing of wafer
- 10. Remove protective resist
 - 1165 Remover, 75 °C, 30 min
 - Rinse in Isopropanol
 - Blowdry with N_2

A.3 Derivation of the advanced fitting function

With the expression of Γ given by equation (2.9) and assuming $R \gg R_0$ we arrive at

$$\Gamma = \frac{1 - \omega^2 L(C + C_c) + j\omega(\frac{L}{R} - R_0 C_c(1 - \omega^2 LC))}{1 - \omega^2 L(C + C_c) + j\omega(\frac{L}{R} + R_0 C_c(1 - \omega^2 LC))} \quad (\text{A.1})$$

Let $x^2 = \left(\frac{\omega}{\omega_0}\right)^2$ and $k = \frac{C}{C+C_c}$ so that

$$\Gamma = \frac{1 - x^2 + jx\omega_0\left(\frac{L}{R} - R_0C_c(1 - x^2\omega_0^2LC)\right)}{1 - x^2 + jx\omega_0\left(\frac{L}{R} + R_0C_c(1 - x^2\omega_0^2LC)\right)} \quad (\text{A.2})$$

Now recall that $Q_{int} = \omega_0R(C + C_c)$ and $Q_{ext} = \frac{C+C_c}{R_0C_c^2\omega_0} = \frac{C}{R_0kC_c^2\omega_0}$, this leads to

$$\begin{aligned} \Gamma &= \frac{1 - x^2 + jx\left(\frac{\omega_0L}{R} - \omega_0R_0C_c + \frac{x^2\omega_0LC}{L(C+C_c)}\right)}{1 - x^2 + jx\left(\frac{\omega_0L}{R} + \omega_0R_0C_c - \frac{x^2\omega_0LC}{L(C+C_c)}\right)} = \frac{1 - x^2 + jx\left(\frac{1}{Q_{int}} + \frac{x^2C-(C+C_c)}{C_cQ_{ext}}\right)}{1 - x^2 + jx\left(\frac{1}{Q_{int}} + \frac{(C+C_c)-x^2C}{C_cQ_{ext}}\right)} \\ &= \frac{1 - x^2 + jx\left(\frac{1}{Q_{int}} - \frac{1-kx^2}{(1-k)Q_{ext}}\right)}{1 - x^2 + jx\left(\frac{1}{Q_{int}} + \frac{1-kx^2}{(1-k)Q_{ext}}\right)} \end{aligned} \quad (\text{A.3})$$

We now take a look at this expression close to the resonance frequency by letting $\omega = \omega_0 + \delta\omega$ and thus we can write $x = \frac{\omega}{\omega_0} = \frac{\omega_0 + \delta\omega}{\omega_0} = 1 + \varepsilon$ where $\varepsilon = \frac{\delta\omega}{\omega_0}$. If we expand $x^2 = (1 + \varepsilon)^2 = (1 + 2\varepsilon + \varepsilon^2)$ and omit the second order term because of $\omega_0 \gg \delta\omega$ and plugging this into equation (A.3) we get

$$\begin{aligned} \Gamma &= \frac{1 - \left(1 + 2\frac{\delta\omega}{\omega_0}\right) + j\left(1 + \frac{\delta\omega}{\omega_0}\right)\left(\frac{1}{Q_{int}} - \frac{1-k(1+2\frac{\delta\omega}{\omega_0})}{(1-k)Q_{ext}}\right)}{1 - \left(1 + 2\frac{\delta\omega}{\omega_0}\right) + j\left(1 + \frac{\delta\omega}{\omega_0}\right)\left(\frac{1}{Q_{int}} + \frac{1-k(1+2\frac{\delta\omega}{\omega_0})}{(1-k)Q_{ext}}\right)} = \\ &= \frac{\delta\omega - j\left(\frac{\omega_0}{2Q_{int}} - \frac{\omega_0}{2Q_{ext}} + \frac{k\delta\omega}{(1-k)Q_{ext}}\right) - j\left(\frac{\delta\omega}{2Q_{int}} - \frac{\delta\omega}{2Q_{ext}} + \frac{k\frac{\delta\omega^2}{\omega_0}}{(1-k)Q_{ext}}\right)}{\delta\omega - j\left(\frac{\omega_0}{2Q_{int}} + \frac{\omega_0}{2Q_{ext}} - \frac{k\delta\omega}{(1-k)Q_{ext}}\right) - j\left(\frac{\delta\omega}{2Q_{int}} + \frac{\delta\omega}{2Q_{ext}} - \frac{k\frac{\delta\omega^2}{\omega_0}}{(1-k)Q_{ext}}\right)} \end{aligned} \quad (\text{A.4})$$

If we now assume that $\frac{\delta\omega}{Q} \ll 1$ we obtain the fitting function given in equation (A.5).

$$\Gamma = \frac{\delta\omega - j\left(\frac{\omega_0}{2Q_{int}} - \frac{\omega_0}{2Q_{ext}}\right)}{\delta\omega - j\left(\frac{\omega_0}{2Q_{int}} + \frac{\omega_0}{2Q_{ext}}\right)} \quad (\text{A.5})$$

Appendix B

Sammanfattning av kandidatarbete Paint it Black

A short resume of the thesis Paint it Black in Swedish.

B.1 Introduktion

Ett av de hetaste ämnena inom modern forskning idag är att försöka realisera en så kallad “kvantdator”, det vill säga, en dator som istället för att använda sig av bitar som är den klassiska datorns byggstenar utnyttjar kvantbitar. En bit kan bara anta de diskreta värdena 0 eller 1 respektive medan en kvantbit utnyttjar egenskapen att den kan anta värdena $|0\rangle$, $|1\rangle$ eller en kvantsuperposition av dessa tillstånd. Teoretiskt sett kan man lösa flera olika problem med kvantdatorer som skulle ta flera år för en klassisk dator att lösa.

Sådana kvantbitar kan realiseras genom att tillverka supraledande kretsar som har anharmoniska energispektrum.

Problemet ligger i att när kvantbitar interagerar med sin omgivning så dekohererar de efter en stund och därmed tappar sina kvantmekaniska egenskaper som gör dem funktionsdugliga. Elektromagnetisk strålning har visat sig vara en av de stora bidragen till korta dekoherens-tider och detta faktum innebär att effektiva metoder för att skölda kvantbitar efterfrågas.

Supraledare i allmänhet påverkas negativt av elektromagnetisk strålning på grund av att de s.k. Cooper-paren (två elektroner i bosoniskt tillstånd) i materialet splittras upp till enstaka oparade elektroner och hål. Dessa kallas för kvasipartiklar och bidrar till förluster i materialets supraledande egenskaper. Detta innebär att alla supraledande komponenter är känsliga för elektromagnetisk strålning.

I detta arbete har vi försökt att skydda komponenten från elektromagnetisk strålning genom att designa en cylindrisk sköld i metall vars insida har täckts av

olika absorbenter. Vi har även placerat några olika absorbenter i provhållarens tak för att se vilken av metoderna som har bäst effekt. För att kunna kvantifiera resultaten av lyckad strålningsreducering har vi valt att mäta egenskaperna hos en supraledande resonator istället för att försöka mäta strålningsnivåerna direkt.

B.2 Teori

B.2.1 Resonatorer

En supraledande resonators förmåga att lagra energi kan beskrivas med en kvalitetsfaktor Q som är ett mått på hur mycket energi som dissiperas per cykel. På grund av att kvasipartiklar ger förluster i komponenten så är kvalitetsfaktorn hos resonatorn ett bra sätt att observera absorbentens förmåga att absorbera EM-strålning. Förhållandet mellan resonatorns kvalitetsfaktor och kvasipartikeldensitet ges av (2.10)[2]. Kvasipartikelalstring som en konsekvens av termiska effekter följer även sambandet $n_{qp} \propto e^{-1/T}$ vilket innebär att när $T \rightarrow 0$ förväntas det att kvasipartiklar försvinner, detta är dock inte sant, då kvasipartiklar genereras även då temperaturen når extremt låga temperaturer som en konsekvens av EM-strålning. En ökning av resonatorns kvalitetsfaktor indikerar alltså att elektromagnetisk strålning som interfererar med resonatorn har reducerats ifall de termiska effekterna kan negligeras. Eftersom experimentet utförs i kryogeniska temperaturer så kan termiska effekter negligeras, och förluster på grund av alstring av kvasipartiklar antas ha sitt ursprung i elektromagnetisk strålning.

Genom att studera reflektionen av inskickad signal till resonatorn kan kvalitetsfaktorn beräknas. Reflektionskoefficienten ges av ekvation(2.9).

B.2.2 Absorbenter

När man designar absorbenter är det i huvudsak två faktorer som är viktiga för materialets skärmningsegenskaper. För det första skall materialet hålla reflekterad strålning till ett minimum och för det andra skall materialet effektivt kunna absorbera strålningen och sedan dissipera den till värme.

Det första kriteriet bestäms av reflektionskoefficienten $\Gamma = (Z - Z_0)/(Z + Z_0)$ där $Z_0 = \sqrt{\mu_0/\epsilon_0} \approx 377 \Omega$ och där Z är absorbentens impedans som bestäms av permittiviteten och permeabiliteten hos materialet. Ifall $Z \approx Z_0$ kommer alltså merparten av strålningen träda in i materialet och dämpas.

Det andra kriteriet fås genom att lösa Maxwells ekvationer i ett material med stora förluster och ingen elektrisk ledningsförmåga. Vi antar att vågen färdas i den positiva x-riktningen och får då lösningar på formen $E_x(z) = E^+ e^{\gamma z}$ för en elektromagnetisk våg som färdas genom ett material med höga förluster och som

inte har någon elektrisk ledningsförmåga. Realdelen av γ bestämmer hur mycket fältstyrkan dämpas och för ett material med sådana egenskaper har γ följande utseende

$$\gamma = \omega(\mu^2 \varepsilon'^2 + \tan^2 \delta)^{1/4} \sin \left(\frac{1}{2} \tan^{-1} \left(\frac{\tan \delta}{\mu \varepsilon'} \right) \right) \quad (\text{B.1})$$

Detta innebär att permittiviteten och permeabiliteten hos materialet måste vara höga för att effektivt kunna dämpa den inträngande strålningen. Dock bestäms även materialets impedans Z av permittiviteten och permeabiliteten enligt $Z = \sqrt{\mu/\varepsilon}$, så även fast materialets förmåga att absorbera strålningen är god så kan en stor del av den inkommande strålningen reflekteras ifall Z skiljer sig från Z_0 .

B.3 Experiment

Resonatorn är placerad på ett chip, detta chip är fastlimmat i provlådan som består av guldpläterat syrefritt koppar, dess olika beståndsdelar visas i figur 3.1a. Vissa absorbenter är av sådan natur att de är svåra att ta bort efter applicering och eftersom provlådan inte får förstöras så kan dessa absorbenter inte appliceras inuti provhållaren. Detta ledde till att en extra sköld designades som skulle vara tillräckligt billigt så att en sköld per absorber skulle kunna tillverkas. Skölden tillverkades utav en 77 mm lång mässingsrundstav av den anledning att mässing är ett billigt och lättillgängligt material som är en god termisk ledare. Lock och ett underrede tillverkades för att kunna användas till alla mätningar och den enda delen som behövdes bytas ut var cylindern. En genomskärning av skölden kan åskådliggöras i figur 3.7.

För att mäta resonatorns kvalitetsfaktor används en Vector Network Analyzer (VNA). Denna utför ett frekvenssvep och mäter sedan Γ . Genom att använda en kurvanpassning till uppmätta datapunkter kan vi extrahera resonatorns kvalitetsfaktor via fas- och magnitudinformationen från Γ .

Fem olika uppställningar har använts i detta arbete, två stycken absorbenter har applicerats på cylinderns insida så att de får ungefär 2 mm tjocklek. Dessa är ECCOSORB 300 samt den egengjorda absorbentern "Magic Mix 'Black Hole'" som består av kiselkarbid av olika kornstorlekar, finmalen kimrök samt ett tvåkomponentslim. Fördelningen av de olika beståndsdelarna finns att åskåda i tabell 3.1. Dessa två absorbenter är av färgliknande natur och härdar efter applicering. De två resterande absorbenterna, ECCOSORB MCS-U-SA samt ECCOSORB GDS-U-SA är kavitsresonans-absorbenter och har applicerats på insidan av provhållaren, direkt ovanför mikrochipet. De kommer i form av ark som är några millimeter tjocka och kan klippas ut till godtyckliga dimensioner. De är även självhäftande och lätta att ta bort ifall så önskas.

Skälet till varför de olika absorberarna har applicerats på olika sätt är helt enkelt att de färgliknande absorberarna är svåra att avlägsna när de väl applicerats. Provhållarens dimensioner gör att det är svårt att applicera färg på ett noggrant sätt, därför är det inte önskvärt att applicera färg-absorberarna inuti provhållaren.

Den femte uppställningen består av en omålad cylinder och används som referens till de andra absorberarna.

B.4 Resultat och diskussion

De uppmätta kvalitetsfaktorerna finns att åskådliggöras i figurerna 4.1-4.3 för NbN-resonatoren samt figurerna 4.6-4.8 för Nb-resonatoren. Vi noterar att referensmätningen har överlägset högst kvalitetsfaktor. Detta är ett otroligt överraskande och oförväntat resultat. Den mest troliga förklaringen till varför vi uppmätte detta resultat är att resonatorchipet som sitter i provhållaren har blivit skadat när vi öppnat provhållaren för att byta absorberer. Andra felkällor kan inkludera att de absorberer vi har placerat i provhållarens tak interagerar med chipet och ändrar dess effektiva dielektricitetskonstant vilket skulle resultera i en förändring av kvalitetsfaktor. Dock skulle det även innebära att resonatorns resonansfrekvens skiftas och denna observation har inte gjorts. En annan teori kan vara att den elektromagnetiska energi som absorberats av de absorberer inuti provhållaren värmt upp chipet och ändrat dess supraledande egenskaper. Men även om så skulle vara fallet skulle detta inte förklara varför vi även uppmäter lägre kvalitetsfaktorer för de absorberer som applicerats på sköldens insida då dessa omöjligt kan interferera med chipet. Ytterligare en referensmätning utfördes efter att detta resultat uppmättes, resultatet för resonatorns kvalitetsfaktor finns att åskådliggöras i figur 4.6 för Nb. I denna figur ser vi att referensmätningarnas relativa skillnad är ungefär 50% vilket indikerar på att resonatorns egenskaper har ändrats mellan mätningarna.

B.5 Slutsats

Vi drar slutsatsen att utav de olika absorberarna som testats är den egengjorda absorberer "Black Hole" antagligen mest effektiv om man bara observerar interna skillnader. Dock behövs fler mätningar för att kunna dra några definitiva slutsatser på grund av motsägelsefull data.

Appendix C

Data sheets

On the following pages the data sheets for the three commercially available absorbers that were used are shown.

ECCOSORB[®] Coating 300

Two Part Polyurethane Coating

Material Characteristics

- Two-Part polyurethane coating that is heavily loaded with iron to provide its absorbing characteristics
- It is a thixotropic coating that can be brushed on or sprayed on using common spray equipment
- Replaces the discontinued Coating 269E

Applications

- ECCOSORB[®] Coating 300 is designed to reduce the radar cross section of objects, to reduce false echo or ghost images on ship radar, and to attenuate surface currents that are generated by radiation impinging on metal surfaces.
- ECCOSORB[®] Coating 300 is designed for use on compound surfaces where flat sheet elastomer or foam absorbers are not desirable.
- To operate as a specular absorber such that resonant absorption at a particular frequency is obtained, it is necessary for the ECCOSORB[®] Coating 300 to be bonded to a metal surface. The overall thickness of the coating is critical to performance as a specular absorber.

Shipping & Availability

- ECCOSORB[®] Coating 300 is available in 2 pound (quart) containers and 8 pound (gallon) containers.
- Both Part A and Part B ship as a hazardous material. Part A ships as a Class 3 Flammable, UN 1993, PG III, and Part B ship as a Class 8 Corrosive, UN2735, PG II.

Thickness Note

- ECCOSORB[®] Coating 300 is applied in thin layers until the correct thickness is obtained. Correct thickness is determined on a case-by-case situation depending on application and frequency of operation.

Instructions for Use

- The system has to be applied in dry conditions
- Make sure that the surface to be coated is clean and free of oil and dusts
- The temperature should be higher than 15 °C during application and curing
- Thoroughly mix the paint until homogeneous
- Add the catalyst in the correct weight ratio, *see Typical Properties Table below*
- Pot Life is 2 hours
- It is recommended to build up the total thickness of the coating in steps of 100 - 150 µm with flash times of one hour between steps. The total layer should be cured for 24 hours minimum at room temperature. For layers thicker than 500 µm, the curing steps should be 24 hours after each 500 µm layer.
- For slightly accelerated curing of the final thickness, 2 hours at 80 °C is recommended. Flash point between layer applications must be maintained to ensure that the solvent has evaporated.
- For thinning, small amount of MEK may be used. Extended flash points are required to evaporate solvent

Typical Properties

Max. Service Temperature, °F (°C)	302 (150)
Frequency Range	1-18 GHz
Color	Dark Gray
Density	4.6 g/cc
Surface weight of 0.7 mm thick coating	3.22 kg/m ²
Mix Ratio, Paint:Catalyst	100:1
Pot Life	2 hours
Recommended thickness of each coating	100 - 150 µm
Shelf Life	6 months

ECCOSORB® GDS

High-Loss Silicone Rubber Sheet

Material Characteristics

- Thin, flexible, electrically non-conductive silicone rubber sheet
- Frequency range from 6 - 35 GHz
- Does not support fungal growth per MIL-STD-810E
- Impervious to moisture and can be subjected to moisture with no adverse effects
- Low out-gassing properties for space applications
- Can be cut and fitted to compound curves

Applications

- When placed within a cavity ECCOSORB® GDS has proven to be very effective at dampening resonances due to the absorbers high permittivity and permeability
- When bonded to a metal surface, ECCOSORB® GDS will significantly reduce the reflectivity of metal objects or structures due to the flow of microwave currents on that surface
- It can be applied to antenna elements, microwave dishes, the inner or outer surfaces of waveguides for isolation, attenuation, or modification of radiating patterns.
- When applied to side or even rear surfaces of certain objects, ECCOSORB® GDS will cause a significant reduction in "head on" reflectivity or backscattering.
- Although not intended as a specular absorber, it will reduce metal plate reflectivity by a few dB.

Instructions for Use

- ECCOSORB® GDS should be bonded to a metal surface for optimal *reflectivity* performance. If a metal surface is not available, it can be supplied upon request with an aluminum foil backing (ML) designated as GDS/ML

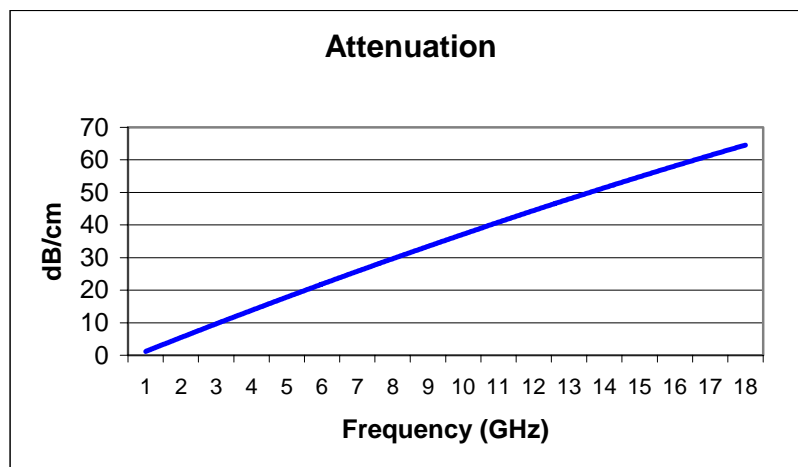
Typical Properties

Electrical Properties taken at 8.6 GHz

Service Temperature	Cryogenic to 350°F (177°C)
Fire Retardancy	UL-94 V1
Specific Gravity (g/cc)	3.6
Volume Resistivity	>10 ¹¹ ohm-cm
Hardness, Shore A	>70
%TML (with SS6M)	0.2 (0.33)
%CVMC (with SS6M)	0.081 (0.09)
Dielectric Constant e'	13
Dielectric Loss Tangent, tan δ _d	0.2
Magnetic Permeability, μ'	1.7
Magnetic Loss Tangent, tan δ _m	0.78
Weight, lbs/ft ² (kg/m ²)	0.6 (2.92)
Weight, lbs/ft ² (kg/m ²) with SS6M PSA	0.7 (3.41)

Availability

- ECCOSORB® GDS is available in sheets 0.030" x 12" x 12" (0.076 cm x 30.5 cm x 30.5 cm)
- Upon special request, ECCOSORB® GDS can be supplied in sheets up to 36" (914.4mm) in length
- It can be supplied with a Pressure Sensitive Adhesive (PSA). Product designation denoting ECCOSORB® GDS with a PSA is ECCOSORB® GDS/SS6M
- ECCOSORB® GDS is available in other sizes and customer specified configurations and thicknesses



EMERSON & CUMING MICROWAVE PRODUCTS, INC., 28 York Avenue, Randolph, MA 02368 / Telephone (781) 961-9600. Use of Information and Material: Values shown are based on testing of laboratory test specimens and represent data that falls within normal range of the material. These values are not intended for use in establishing maximum, minimum or ranges of values for specification purposes. Any determination of the suitability of the material for any purpose contemplated by the user and the manner of such use is the responsibility of the user. The user should determine that the material meets the needs of the user's product and use. We hope that the information given here will be helpful. It is based on data and knowledge considered to be true and accurate and is offered for the user's consideration, investigation and verification but we do not warrant the results to be obtained. Please read all statements, recommendations or suggestions in conjunction with our conditions of sale INCLUDING THOSE LIMITING WARRANTIES AND REMEDIES, which apply to all goods supplied by us. We assume no responsibility for the use of these statements, recommendations or suggestions nor do we intend them as a recommendation for any use, which would infringe any patent or copyright. Emerson & Cuming Microwave Products Inc.

ECCOSORB[®] MCS

Thin, Flexible, Broadband Absorbers

Material Characteristics

- Thin, flexible, high-loss, magnetically loaded, electrically non-conductive silicone rubber sheet
- Frequency range from 800 MHz to 18 GHz
- Impervious to moisture and can be subjected to outdoor environments and high altitudes, including space, with no adverse effects
- Low out-gassing properties for space applications
- Can be cut and fitted to compound curves

Applications

- When placed within a cavity ECCOSORB[®] MCS has proven to be very effective at dampening resonances due to the absorbers high permittivity and permeability as well as high loss values, which in turn reduces the overall VSWR
- ECCOSORB[®] MCS is designed for the suppression of surface currents over a wide range of frequencies
- Useful for the suppression of creeping waves and reduction of cavity resonances in microwave modules.
- ECCOSORB[®] MCS is also useful in reducing RF coupling of antennas and microwave components

Availability

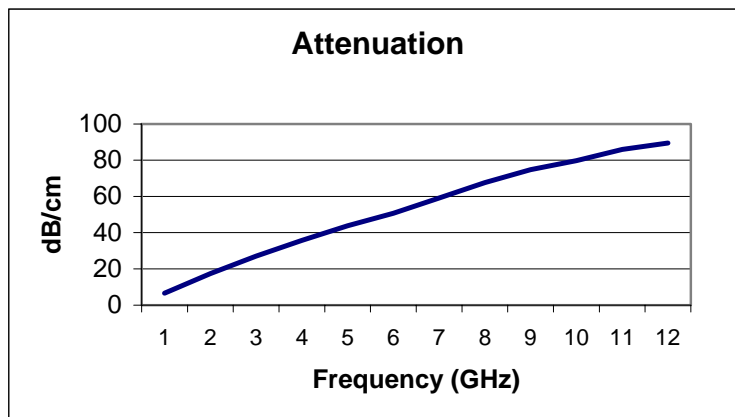
- ECCOSORB[®] MCS is available in sheets 0.040" x 12" x 12" (0.101cm x 30.5cm x 30.5cm)
- Upon special request, ECCOSORB[®] MCS can be supplied in sheets up to 36" (914.4mm) in length
- It can be supplied with a Pressure Sensitive Adhesive (PSA). Product designation denoting ECCOSORB[®] MCS with a PSA is ECCOSORB[®] MCS/SS6M
- ECCOSORB[®] MCS is available in other sizes and customer specified configurations and thicknesses upon request

Instructions for Use

- ECCOSORB[®] MCS can be bonded to itself to make thicker sheets or to other substrates with either the factory installed PSA (SS6M), or STYCAST[®] 4952 along with Primer S-11

Typical Properties

Service Temperature, °F (°C)	Cryogenic to 350 (177)
Volume Resistivity	2 x 10 ⁸ ohm-cm
Relative Impedance	0.66 - 0.23
Dielectric Strength, volts/mil	>20
Nominal Thickness, inches (mm)	.040 (1.0)
Hardness, Shore A	>80
Tensile Strength, psi	>500
Elongation, %	>20
Thermal Conductivity, (cal)(cm)/(sec)(cm ²)(°C) (BTU)(in)/(hr)(ft ²)(°F)	0.0028 8.5
Fire Retardancy	UL-94 V1
%TML (with SS6M)	0.3 (0.23)
%CVCM (with SS6M)	0.05 (0.05)
Weight, lb/ft ² (kg/m ²)	0.9 (4.39)
Weight, lb/ft ² (kg/m ²) with SS6M PSA	1.0 (4.87)



EMERSON & CUMING MICROWAVE PRODUCTS, INC., 28 York Avenue, Randolph, MA 02368 / Telephone (781) 961-9600. Use of Information and Material: Values shown are based on testing of laboratory test specimens and represent data that falls within normal range of the material. These values are not intended for use in establishing maximum, minimum or ranges of values for specification purposes. Any determination of the suitability of the material for any purpose contemplated by the user and the manner of such use is the responsibility of the user. The user should determine that the material meets the needs of the user's product and use. We hope that the information given here will be helpful. It is based on data and knowledge considered to be true and accurate and is offered for the user's consideration, investigation and verification but we do not warrant the results to be obtained. Please read all statements, recommendations or suggestions in conjunction with our conditions of sale INCLUDING THOSE LIMITING WARRANTIES AND REMEDIES, which apply to all goods supplied by us. We assume no responsibility for the use of these statements, recommendations or suggestions nor do we intend them as a recommendation for any use, which would infringe any patent or copyright. Emerson & Cuming Microwave Products Inc.